Quasinormal modes of the Schwarzschild black hole with arbitrary spin fields

Qiyuan Pan Jiliang Jing*

Institute of Physics and Department of Physics,

Hunan Normal University,

Changsha, Hunan 410081, P. R. China

Abstract

The quasinormal modes (QNMs) associated with the decay of massless arbitrary spin fields around a Schwarzschild black hole are investigated by using the continued fraction method in a united form and their universal properties are found. It is shown that these QNMs become evenly spaced for large angular quantum number l (for the boson perturbations) and j (for the fermion perturbations) and the spacing is independent of the spin number s and overtone number n, and in the complex plane they have an interesting trend which depends on n before they become the same value with the increasing l (or j). It is also shown that the angular quantum number has the surprising effect of increasing real part of the QNMs, but it almost does not affect imaginary part, especially for the lowest lying mode. In addition, the spacing for imaginary part of the QNMs at high overtones is equidistant and equals to $-i/4M$, which is independent of l (or j) and s.

Keywords: Black hole, arbitrary spin fields, quasinormal modes.

PACS numbers: 04.70.-s, 04.50.+h, 11.15.-q, 11.25.Hf

*Corresponding author, Email: jljing@hunnu.edu.cn

I. INTRODUCTION

The evolution of the external field perturbation around a black hole is dominated by three stages [1]: the initial wave burst, the damped oscillations called QNMs and the power-law tail behavior of the waves at very late time. The QNMs have become astrophysically significant with the realistic possibility of gravitational wave detection because they provide us the information about the main parameters of a black hole such as its mass M, charge Q and angular momentum per unit mass $a \equiv J/M$ [2]. In addition, the study of the QNMs can lead to a deeper understanding of the thermodynamic properties of black holes in loop quantum gravity [3] [4], and the QNMs of anti-de Sitter black holes have a direct interpretation in terms of the dual conformal field theory [5] [6] [7].

Regge and Wheeler first studied the linear perturbations of static black holes in 1957 [8]. This pioneering work on this topic has led to many investigations concerning the evolution of various fields in different black holes. Vishveshwara [9] and Press [10] first found the QNMs through numerical computations of the time evolution of the gravitational waves around the black hole. Chandrasekhar and Detweiler proposed the first approach for calculating the QNMs numerically and gave the values of the first few least-damped QNMs [11]. In 1985, Leaver [12] presented a continued fraction method used for calculating the QNMs of both static and rotating black holes. Then, Onozawa et al improved this method for the extreme case in 1996 [13]. The continued fraction method provides extremely accurate values for the QNMs of each black hole which involves the scalar, electromagnetic and gravitational perturbations [14, 15]. Recently it was extended to compute the QNMs of the Dirac field [16, 17]. However, as far as we know nobody use this method to study the Rarita-Schwinger perturbations around a black hole.

Nowadays, it seems that people are searching some possible way to deal with the QNMs of any spacetime with arbitrary spin fields in a united form [18–21]. When we compute the QNMs of the Dirac field perturbations around a black hole, we found that the wave functions and potentials of the Dirac field in the static and rotating spacetimes can be expressed as new forms [17][22]. Starting from the new wave functions and potentials, we can easily extend the continued fraction method to calculate the QNMs associated with the decay of massless scalar ($s = 0$), Dirac ($s = \pm 1/2$), electromagnetic ($s = \pm 1$), Rarita-Schwinger ($s = \pm 3/2$) and gravitational ($s = \pm 2$) perturbations around a Schwarzschild black hole in a united form. The main purpose of this paper is to calculate the QNMs associated with the decay of massless boson and fermion perturbations around a Schwarzschild black hole using the continued fraction method and to find universal properties of the QNMs of these perturbations.

The organization of this paper is as follows. In Sec.2 the wave equations of the Schwarzschild black hole with arbitrary spin fields are obtained by using Newman-Penrose formalism. In Sec.3 a short description of the continued fraction method is given. In Sec. 4 the numerical results for the QNMs of the Schwarzschild black hole with arbitrary spin fields are presented. Last section is devoted to a summary and conclusion.

II. WAVE EQUATIONS OF THE SCHWARZSCHILD BLACK HOLE

In the Boyer-Lindquist coordinates (t, r, θ, φ), the metric for the Schwarzschild black hole is given by

$$ds^2 = \frac{\Delta_r}{r^2}dt^2 - \frac{r^2}{\Delta_r}dr^2 - r^2(d\theta^2 + sin^2\theta d\varphi^2), \tag{2.1}$$

where $\Delta_r = r^2 - 2Mr$ and M represents the mass of the black hole . Throughout this paper we use $G = c = 1$. The null tetrad of this black hole can be taken as

$$\begin{aligned} l^\mu &= (\frac{r^2}{\Delta_r},\ 1,\ 0,\ 0), \\ n^\mu &= \frac{1}{2}(1,\ \ -\frac{\Delta_r}{r^2},\ 0,\ 0), \\ m^\mu &= \frac{1}{\sqrt{2}r}\left(0,\ 0,\ 1, \frac{i}{sin\theta}\right). \end{aligned} \tag{2.2}$$

Assuming that the azimuthal and time dependence of our fields will be the form $e^{-i(\omega t - m\varphi)}$, we find that the derivative operators are

$$\begin{aligned} &D \equiv l^\mu\partial_\mu = \mathcal{D}_0, \quad \Delta \equiv n^\mu\partial_\mu = -\frac{\Delta_r}{2r^2}\mathcal{D}_0^\dagger, \\ &\delta \equiv m^\mu\partial_\mu = \frac{1}{\sqrt{2}r}\mathcal{L}_0^\dagger, \quad \delta^* \equiv m^{*\mu}\partial_\mu = \frac{1}{\sqrt{2}r}\mathcal{L}_0, \end{aligned} \tag{2.3}$$

where

$$\begin{aligned} &\mathcal{D}_n = \frac{\partial}{\partial r} - \frac{iK}{\Delta_r} + \frac{n}{\Delta_r}\frac{d\Delta_r}{dr}, \quad \mathcal{D}_n^\dagger = \frac{\partial}{\partial r} + \frac{iK}{\Delta_r} + \frac{n}{\Delta_r}\frac{d\Delta_r}{dr}, \\ &\mathcal{L}_n = \frac{\partial}{\partial\theta} + \frac{m}{\sin\theta} + n\cot\theta, \quad \mathcal{L}_n^\dagger = \frac{\partial}{\partial\theta} - \frac{m}{\sin\theta} + n\cot\theta, \quad K = r^2\omega. \end{aligned} \tag{2.4}$$

Using the Newman-Penrose formalism [23], we can easily obtain the separated equations for massless scalar, Dirac, electromagnetic, Rarita-Schwinger and gravitational perturbations around a Schwarzschild black hole [17] [24] [25]

$$[\Delta_r\mathcal{D}_{1-s}\mathcal{D}_0^\dagger + 2(2s-1)i\omega r - (A_s + 2s)]\Delta_r^s R_s = 0, \tag{2.5}$$

$$[\mathcal{L}_{1-s}^\dagger\mathcal{L}_s + (A_s + 2s)]S_s = 0, \tag{2.6}$$

with the spin number $s = 0,\ +1/2,\ +1,\ +3/2$ and $+2$;

$$[\Delta_r\mathcal{D}_{1+s}^\dagger\mathcal{D}_0 + 2(2s+1)i\omega r - A_s]R_s = 0, \tag{2.7}$$

$$(\mathcal{L}_{1+s}\mathcal{L}^{\dagger}_{-s} + A_s)S_s = 0, \tag{2.8}$$

with $s = -1/2,\ -1,\ -3/2$ and -2. A_s is the angular separation constant which can be determined analytically for the boson perturbations [26–28]

$$A_s = (l-s)(l+s+1), \qquad l = |s|, |s|+1, \cdots; \tag{2.9}$$

for the fermion perturbations

$$A_s = (j-s)(j+s+1), \qquad j = |s|, |s|+1, \cdots, \tag{2.10}$$

where l and j both are the quantum number characterizing the angular distribution for the boson and fermion perturbations respectively.

Introducing an usual tortoise coordinate

$$dr_* = \frac{r^2}{\Delta_r}dr \tag{2.11}$$

and resolving the equation in the form

$$R_s = \frac{\Delta_r^{-s/2}}{r}\Psi_s, \tag{2.12}$$

we can rewrite the radial Eqs. (2.5) and (2.7) as

$$\frac{d^2\Psi_s}{dr_*^2} + [\omega^2 - V_s(r)]\Psi_s = 0, \tag{2.13}$$

where

$$V_s(r) = is\omega r^2\frac{d}{dr}\left(\frac{\Delta_r}{r^4}\right) + \frac{1}{r^4}\left[(s+A_s)\Delta_r + \left(\frac{s}{2}\frac{d\Delta_r}{dr}\right)^2\right] - \frac{\Delta_r}{r^3}\frac{d}{dr}\left[\Delta_r\frac{d}{dr}\left(\frac{1}{r}\right)\right]. \tag{2.14}$$

with $s = 0,\ \pm 1/2,\ \pm 1,\ \pm 3/2$ and ± 2. Thus, we will study the QNMs of the Schwarzschild black hole with arbitrary spin fields from Eqs. (2.13) and (2.14).

III. THE CONTINUED FRACTION METHOD

It is well known that the quasinormal frequencies are defined to be the modes with purely ingoing waves at the event horizon and purely outgoing waves at infinity [11]. The boundary conditions of the wave function Ψ_s at the event horizon ($r = r_+$) and infinity ($r \to +\infty$) for the Schwarzschild black hole can be given by

$$\Psi_s \sim \begin{cases} (r-r_+)^{-\frac{s}{2}-i\omega r_+}, & r \to r_+; \\ r^{-s+i\omega r_+}e^{i\omega r}, & r \to +\infty. \end{cases} \tag{3.1}$$

A solution to Eq. (2.13) which satisfies the desired behavior at the boundary can be written as

$$\Psi_s = r^{-\frac{s}{2}+2i\omega r_+}(r-r_+)^{-\frac{s}{2}-i\omega r_+}e^{i\omega r}\sum_{n=0}^{\infty} a_n \left(\frac{r-r_+}{r}\right)^n . \tag{3.2}$$

The sequence of the expansion coefficients a_n is determined by a three-term recurrence relation starting with $a_0 = 1$:

$$\begin{aligned} &\alpha_0 a_1 + \beta_0 a_0 = 0, \\ &\alpha_n a_{n+1} + \beta_n a_n + \gamma_n a_{n-1} = 0, \quad n = 1, 2, ... \end{aligned} \tag{3.3}$$

where the recurrence coefficients α_n, β_n, and γ_n are given in terms of n and the black-hole physical parameters by

$$\begin{aligned} \alpha_n &= n^2 + (C_0+1)n + C_0, \\ \beta_n &= -2n^2 + (C_1+2)n + C_3, \\ \gamma_n &= n^2 + (C_2-3)n + C_4 - C_2 + 2, \end{aligned} \tag{3.4}$$

with

$$\begin{aligned} C_0 &= -s + 1 - 2i\omega r_+, \\ C_1 &= -4 + 8i\omega r_+, \\ C_2 &= s + 3 - 4i\omega r_+, \\ C_3 &= -s - 1 + 4i\omega r_+ + 8\omega^2 r_+^2 - A_s, \\ C_4 &= s + 1 - 2(s+2)i\omega r_+ - 4\omega^2 r_+^2. \end{aligned} \tag{3.5}$$

The radial series solution (3.2) converges and the boundary conditions (3.1) are satisfied as the frequency ω is a root of the three-term continued fraction equation [12, 13]

$$0 = \beta_0 - \frac{\alpha_0\gamma_1}{\beta_1-}\frac{\alpha_1\gamma_2}{\beta_2-}\frac{\alpha_2\gamma_3}{\beta_3-}\frac{\alpha_3\gamma_4}{\beta_4-}\cdots . \tag{3.6}$$

So we will calculate the QNMs of the Schwarzschild black hole with arbitrary spin fields using the continued fraction method first proposed by Leaver with this united three-term recurrence relation (3.6).

IV. NUMERICAL RESULTS

In order to compare with other authors' results, we set $r_+ = 2M = 1$. Since Eqs. (2.5) and (2.7) are proportional to complex-conjugate equations, it will suffice to study $s = 0, \ -1/2, \ -1, \ -3/2$ and -2 only. In this section we present the numerical results of the QNMs of the Schwarzschild black hole with arbitrary spin fields obtained by using the numerical approach just outlined in the previous section. The results will be organized into two subsections: the large angular quantum number and high overtones. We note that our results are in good agreement with the Shu's and Cho's results which are obtained by the WKB approach if we take $M = 1$ [18, 32].

A. Large angular quantum number

The fundamental QNMs (n=0) with arbitrary spin fields for $k = 1$ to $k = 30$ are listed in the Table I ($k = l$ for the boson perturbations and $k = j + 1/2$ for the fermion perturbations). Figs. 1 and 2 show that $\Delta\omega = \omega_{k+1} - \omega_k$ as a function of k for the first 4 QNMs with arbitrary spin fields. From the table and figures we know that the QNMs become evenly spaced for large k and the spacing is given by

$$\Delta\omega = \frac{2}{3\sqrt{3}} - 0.0000i, \tag{4.1}$$

which is independent of s and n. This numerical result confirms the analytical work which was first presented by Ferrari and Mashhoon [29, 30].

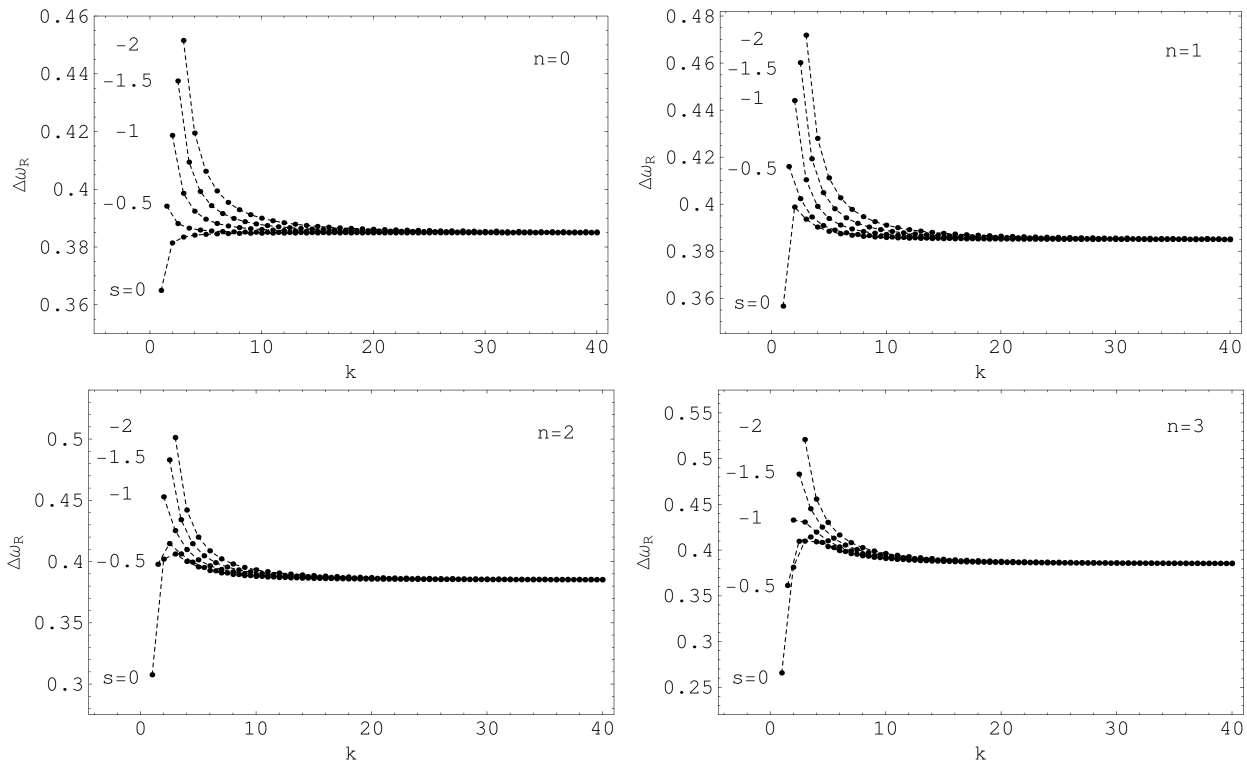

FIG. 1: The spacing $\Delta\omega_R$ as the functions of k for the first 4 QNMs with arbitrary spin fields. In each panel, the five dashed lines from the top to the bottom correspond to $s = -2, \ -3/2, \ -1, \ -1/2$ and 0 respectively. These panels shows that the spacing of the real part is $0.3849 = \frac{2}{3\sqrt{3}}$ for large k.

TABLE I: Fundamental quasinormal frequencies of the Schwarzschild black hole with $k = 0$ to $k = 30$ for the boson perturbations ($k = l$) and $j = 0.5$ to $j = 29.5$ for the fermion perturbations ($k = j + 1/2$).

k	ω_0	ω_{-1}	ω_{-2}	$\omega_{-1/2}$	$\omega_{-3/2}$
0	0.220910-0.209791i				
1	0.585872-0.195320i	0.496527-0.184975i		0.365926-0.193965i	
2	0.967288-0.193518i	0.915191-0.190009i	0.747343-0.177925i	0.760074-0.19281i	0.622583-0.180174i
3	1.35073-0.192999i	1.31380-0.191232i	1.19889-0.185406i	1.14819-0.192610i	1.06010-0.187501i
4	1.73483-0.192783i	1.70619-0.191720i	1.61836-0.188328i	1.53471-0.192540i	1.46950-0.189757i
5	2.11922-0.192674i	2.09583-0.191963i	2.02459-0.189741i	1.92059-0.192507i	1.86873-0.190752i
6	2.50377-0.192610i	2.48399-0.192102i	2.42402-0.190532i	2.30614-0.192490i	2.26306-0.191281i
7	2.88842-0.192570i	2.87128-0.192189i	2.81947-0.191019i	2.69150-0.192479i	2.65465-0.191595i
8	3.27312-0.192544i	3.25801-0.192247i	3.21239-0.191341i	3.07675-0.192473i	3.04455-0.191798i
9	3.65787-0.192525i	3.64435-0.192288i	3.60359-0.191565i	3.46192-0.192468i	3.43332-0.191936i
10	4.04264-0.192512i	4.03041-0.192317i	3.99358-0.191728i	3.84704-0.192464i	3.82132-0.192034i
11	4.42744-0.192501i	4.41627-0.192339i	4.38267-0.191849i	4.23212-0.192462i	4.20874-0.192107i
12	4.81225-0.192493i	4.80198-0.192356i	4.77108-0.191942i	4.61717-0.192462i	4.59575-0.192162i
13	5.19708-0.192487i	5.18757-0.19237i	5.15897-0.192015i	5.00219-0.192459i	4.98243-0.192205i
14	5.58191-0.192482i	5.57306-0.192381i	5.54645-0.192073i	5.38720-0.192457i	5.36885-0.192239i
15	5.96676-0.192478i	5.95848-0.192389i	5.93359-0.192121i	5.77220-0.192456i	5.75507-0.192266i
16	6.35161-0.192475i	6.34383-0.192396i	6.32046-0.192160i	6.15718-0.192456i	6.14112-0.192288i
17	6.73647-0.192472i	6.72913-0.192402i	6.70710-0.192192i	6.54215-0.192455i	6.52704-0.192307i
18	7.12133-0.192470i	7.11439-0.192407i	7.09355-0.192219i	6.92711-0.192455i	6.91285-0.192322i
19	7.50619-0.192468i	7.49961-0.192412i	7.47985-0.192242i	7.31207-0.192454i	7.29856-0.192335i
20	7.89106-0.192466i	7.88480-0.192415i	7.86600-0.192262i	7.69702-0.192454i	7.68419-0.192347i
21	8.27593-0.192465i	8.26997-0.192418i	8.25204-0.192279i	8.08197-0.192453i	8.06974-0.192356i
22	8.66081-0.192463i	8.65511-0.192421i	8.63798-0.192294i	8.46691-0.192453i	8.45524-0.192365i
23	9.04569-0.192462i	9.04022-0.192424i	9.02383-0.192307i	8.85185-0.192453i	8.84069-0.192372i
24	9.43056-0.192461i	9.42533-0.192426i	9.40960-0.192319i	9.23679-0.192453i	9.22609-0.192378i
25	9.81544-0.192461i	9.81041-0.192428i	9.79531-0.192329i	9.62172-0.192452i	9.61145-0.192384i
26	10.2003-0.192460i	10.1955-0.192429i	10.1809-0.192338i	10.0067-0.192452i	9.99678-0.192389i
27	10.5852-0.192459i	10.5805-0.192431i	10.5665-0.192346i	10.3916-0.192452i	10.3821-0.192393i
28	10.9701-0.192458i	10.9656-0.192432i	10.9521-0.192353i	10.7765-0.192452i	10.7673-0.192397i
29	11.3550-0.192458i	11.3506-0.192433i	11.3376-0.192359i	11.1614-0.192452i	11.1526-0.192401i
30	11.7399-0.192457i	11.7357-0.192434i	11.7230-0.192365i	11.5464-0.192452i	11.5378-0.192404i

Motivated by Eq. (4.1), we further investigate the QNMs with arbitrary spin fields for large angular quantum number. Fig. 3 shows the behavior of the first 4 QNMs with arbitrary spin fields for $k = 1$ to $k = 40$. We find that in the complex plane these QNMs have an interesting trend before they become the same value with the increasing k. For $n = 0$ the QNMs with $s = 0$ and $-1/2$ will tend

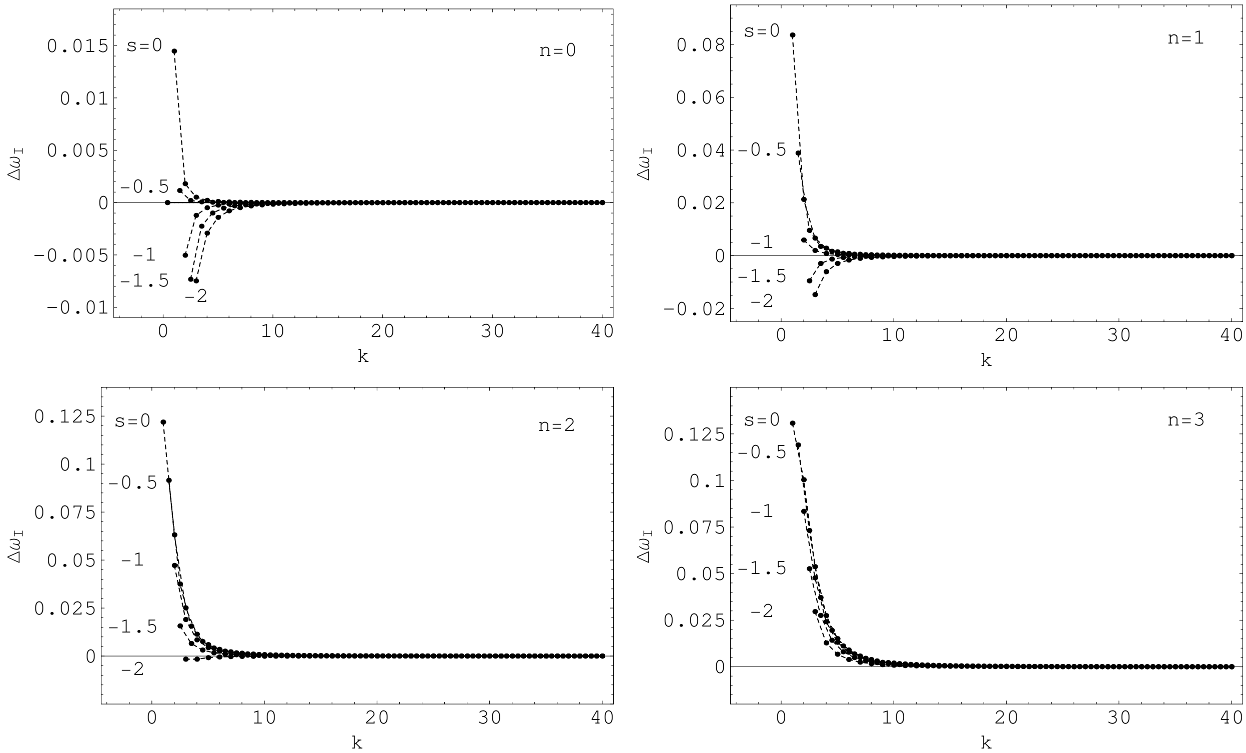

FIG. 2: The spacing $\Delta\omega_I$ as the functions of k for the first 4 QNMs with arbitrary spin fields. In each panel, the five dashed lines from the top to the bottom correspond to $s = 0, \ -1/2, \ -1, \ -3/2$ and -2 respectively. These panels shows that the spacing of the imaginary part becomes zero for large k.

to the same value from the bottom which are contrary to those with $s = -1, \ -3/2$ and -2. But for $n = 1$ the QNMs with $s = 0, \ -1/2$ and -1 will tend to the same value from the bottom which are different from those with $s = -3/2$ and -2. For $n = 2$ the QNMs with $s = 0, \ -1/2, \ -1$ and $-3/2$ will tend to the same value from the bottom except $s = -2$. For $n \geq 3$ the QNMs with arbitrary spin fields all tend to the same value from the bottom.

From the Table I and Fig. 3 we learn that the real part of this same value only depends on k and the imaginary part only depends on n for large angular quantum number and the distribution can be expressed as (for the cases $n \ll k$)

$$\omega_n \approx \frac{2}{3\sqrt{3}}\left[l(orj) + \frac{1}{2} - (n + \frac{1}{2})i\right], \tag{4.2}$$

which is independent of s. This numerical result agrees with the Ferrari and Mashhoon's analytical work [29, 30].

B. High overtones

There is a great deal of effort which has been contributed to compute the QNMs of the Schwarzschild black hole for the boson and Dirac perturbations [2, 12, 17–21, 29–32]. But the Rarita-

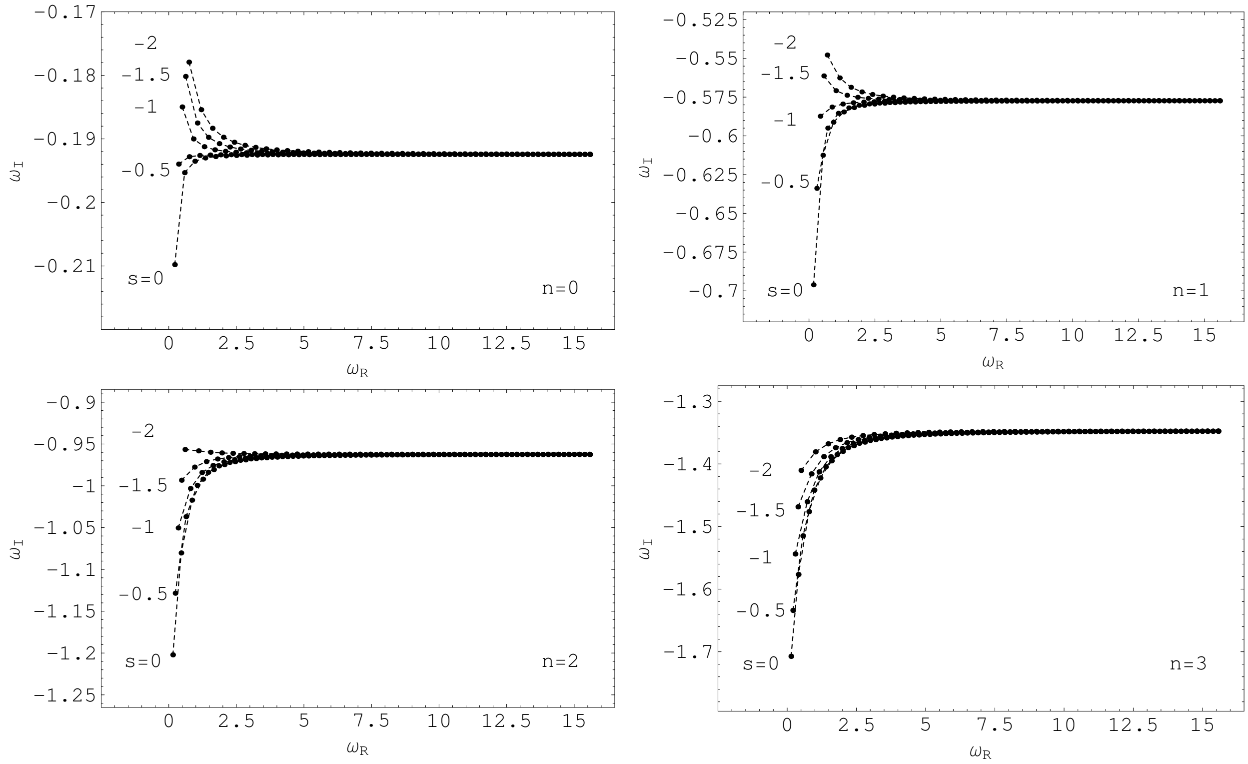

FIG. 3: Graphs of the first 4 QNMs with arbitrary spin fields for $k = 1$ to $k = 40$. In each panel, the five dashed lines from the top to the bottom correspond to the modes for $s = -2$, $-3/2$, -1, $-1/2$ and 0 respectively.

Schwinger perturbations around the Schwarzschild black hole have not been computed by using the continued fraction method. Therefore, we will study the gravitino QNMs ($s = -3/2$) for the high overtones in this subsection.

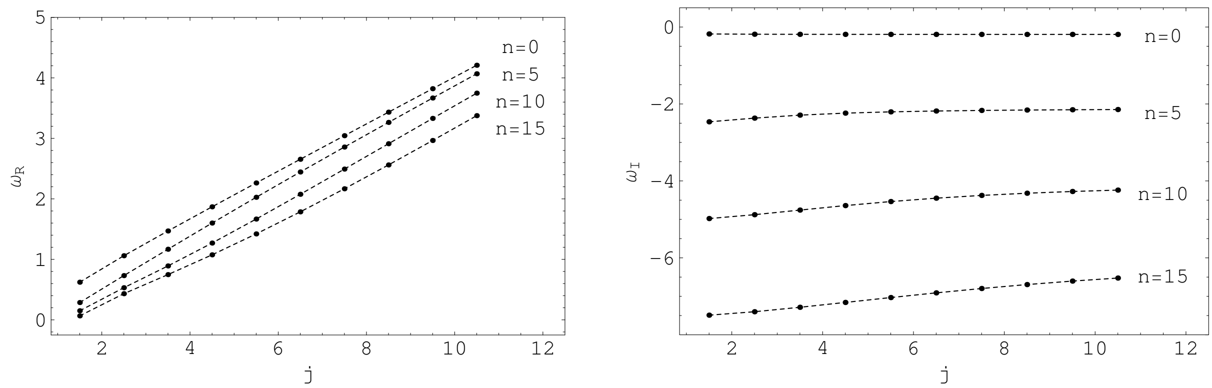

FIG. 4: Dependence of the gravitino QNMs ($s = -3/2$) on j for the Schwarzschild black hole. The left figure shows that j has the surprising effect of increasing real part ω_R, and the right one shows that it almost does not affect imaginary part ω_I, especially for the lowest lying mode.

The gravitino QNMs of the Schwarzschild black hole for $j = 1.5$ to $j = 5.5$ and $n = 1$ to $n = 15$ are given by Table II and their dependence on j is described by Fig. 4. We learn from Table I-II and Fig. 4 that j has the surprising effect of increasing real part of the gravitino QNMs, but it almost

TABLE II: Gravitino quasinormal frequencies of the Schwarzschild black hole for $j = 1.5$ to $j = 5.5$ and $n = 1$ to $n = 15$.

n	$\omega \quad (j = 1.5)$	$\omega \quad (j = 2.5)$	$\omega \quad (j = 3.5)$	$\omega \quad (j = 4.5)$	$\omega \quad (j = 5.5)$
1	0.562595-0.561302i	1.02278-0.570846i	1.44209-0.573812i	1.84700-0.575121i	2.24505-0.575815i
2	0.473382-0.993289i	0.956371-0.977592i	1.39057-0.971049i	1.80520-0.967913i	2.20995-0.966192i
3	0.393367-1.46850i	0.876418-1.41586i	1.32163-1.38829i	1.74668-1.37405i	2.15970-1.36600i
4	0.332719-1.96285i	0.798736-1.88258i	1.24433-1.82858i	1.67643-1.79704i	2.09720-1.77823i
5	0.286619-2.46360i	0.731529-2.36818i	1.16735-2.29023i	1.60027-2.23823i	2.02614-2.20485i
6	0.250036-2.96630i	0.675875-2.86411i	1.09639-2.76845i	1.52373-2.69655i	1.95060-2.64651i
7	0.219764-3.46949i	0.629985-3.36518i	1.03371-3.25794i	1.45085-3.16924i	1.87437-3.10250i
8	0.193842-3.97265i	0.591705-3.86865i	0.979327-3.75448i	1.38387-3.65289i	1.80045-3.57103i
9	0.171028-4.47564i	0.559259-4.37316i	0.932298-4.25522i	1.32354-4.14436i	1.73079-4.04982i
10	0.150495-4.97842i	0.531316-4.87804i	0.891450-4.75839i	1.26971-4.64118i	1.66639-4.53656i
11	0.131664-5.48101i	0.506902-5.38295i	0.855700-5.26291i	1.22178-5.14154i	1.6075-5.02923i
12	0.114113-5.98343i	0.485303-5.88772i	0.824139-5.76813i	1.17903-5.64420i	1.55396-5.52619i
13	0.0975169-6.48571i	0.465986-6.39228i	0.796036-6.27366i	1.14074-6.14832i	1.50536-6.02622i
14	0.0816168-6.98791i	0.448546-6.89660i	0.770808-6.77929i	1.10628-6.65333i	1.46120-6.52838i
15	0.0661918-7.49005i	0.432674-7.40066i	0.747993-7.28486i	1.07509-7.15888i	1.42098-7.03202i

does not affect imaginary part, especially for the lowest lying mode. The conclusion is also true for other perturbations [2, 12, 17, 29–32].

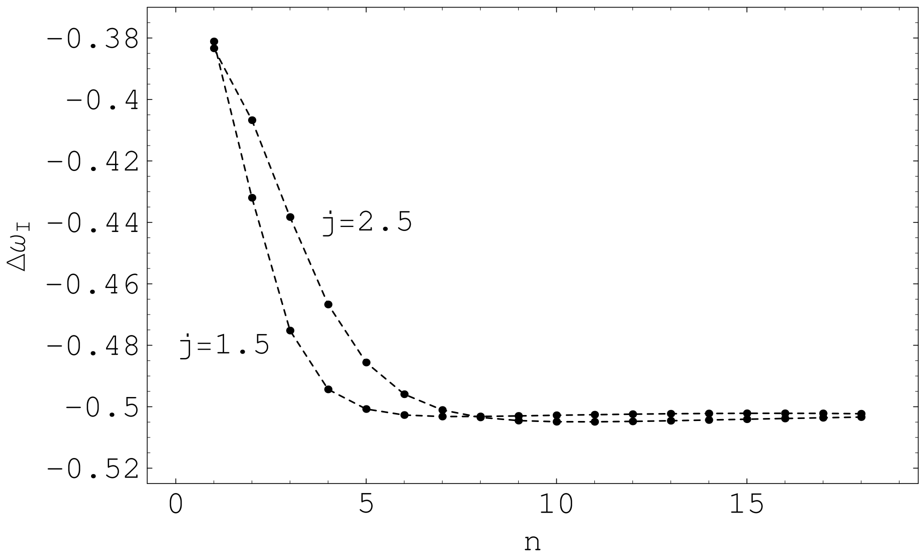

FIG. 5: The spacing $\Delta\omega_I$ versus overtone number n with $j = 1.5$ and 2.5 for the gravitino QNMs. The figure shows that $\Delta\omega_I \approx -1/4M$ for large n.

From Table II and Fig. 5 we know that the gravitino QNMs for $j = 1.5$ and 2.5 demonstrate the following asymptotic behavior

$$Im(\omega_{n+1}) - Im(\omega_n) \approx -\frac{i}{4M}, \quad \text{as} \quad n \to \infty, \tag{4.3}$$

which is the same as that of the boson and Dirac perturbations [2, 12, 17]. This conclusion not only confirms the results which are obtained by the analytical approaches [19–21], but also resolves the controversy on the spacing for the imaginary part of the QNMs for the spin-1/2 field [16, 17]. Thus, we can conclude that the spacing for imaginary part of the QNMs at high overtones is $-i/4M$ which is independent of l (or j) and s.

V. SUMMARY

The wave equations for the boson and fermion perturbations in the Schwarzschild black hole spacetime are obtained by means of the Newman-Penrose formulism. Then, the QNMs of this black hole with arbitrary spin fields are evaluated by using the continued fraction method. Five universal properties of the QNMs for these perturbations are listed in the following: (i) These QNMs become evenly spaced for large angular quantum number l (for the boson perturbations) and j (for the fermion perturbations) and the spacing is given by $\Delta\omega = \frac{2}{3\sqrt{3}} - 0.0000i$, which is independent of s and n. (ii) These QNMs have an interesting trend which depends on n before they become the same value with the increasing k in the complex plane. (iii) The distribution of the QNMs for large values l (or j) and small n can be written by $\omega_n \approx \frac{2}{3\sqrt{3}}\left[l(orj) + \frac{1}{2} - (n + \frac{1}{2})i\right]$, which is independent of s. (iv) The angular quantum number l (or j) has the surprising effect of increasing real part of the QNMs, but it almost does not affect imaginary part, especially for the lowest lying mode. (v) The QNMs also become evenly spaced for large n and the spacing for the imaginary part is equidistant and equals to $-i/4M$, which is independent of l (or j) and s.

Acknowledgments

This work was supported by the National Natural Science Foundation of China under Grant No. 10473004; the FANEDD under Grant No. 200317; and the SRFDP under Grant No. 20040542003.

[1] V. P. Frolov and I. D. Novikov, *Black hole physics: basic concepts and new developments* (Dordrecht: Kluwer Academic), 1998.

[2] K. Kokkotas and B. Schmidt, Living Reviews Relativ. **2**, 2 (1999).

[3] S. Hod, Phys. Rev. Lett. **81**, 4293 (1998).

[4] O. Dreyer, Phys. Rev. Lett. **90**, 081301 (2003).

[5] J. M. Maldacena, Adv. Theor. Math. Phys. **2**, 231 (1998).

[6] E. Witten, Adv. Theor. Math. Phys. **2**, 253 (1998).

[7] S. Kalyana Rama and B. Sathiapalan, Mod. Phys. Lett. A **14**, 2635 (1999).

[8] T. Regge and J. Wheeler, Phys. Rev. **108**, 1063 (1957).

[9] C. V. Vishveshwara, Nature (London) **227**, 936 (1970).

[10] W. Press, Astrophys. J. **170**, L105 (1971).

[11] S. Chandrasekhar and S. Detweller, Proc. R. Soc. Lond. A **344**, 441 (1975).

[12] E. W. Leaver, Proc. R. Soc. Lond. A **402**, 285 (1985).

[13] H. Onozawa, T. Mishima, T. Okamura and H. Ishihara, Phys. Rev. D **53**, 7033 (1996).

[14] E. Berti, V. Cardoso and S. Yoshida, Phys. Rev. D **69**, 124018 (2004).

[15] E. Berti and K. D. Kokkotas, Phys. Rev. D **71**, 124008 (2005).

[16] K. H. C. Castello-Branco, R. A. Konoplya and A. Zhidenko, Phys. Rev. D **71**, 047502 (2005).

[17] Jiliang Jing, Phys. Rev. D **71**, 124006 (2005); gr-qc/0502023.

[18] Fu-Wen Shu and You-Gen Shen, Phys. Lett. B **619**, 340 (2005).

[19] H. T. Cho, Phys. Rev. D **73**, 024019 (2006).

[20] I. B. Khriplovich and G. Y. Ruban, gr-qc/0511056.

[21] S. Musiri and G. Siopsis, Class. Quant. Grav. **20**, L285 (2003).

[22] Jiliang Jing, Phys. Rev. D **71**, 124011 (2005).

[23] E. Newman and R. Penrose, J. Math. Phys. (N. Y.) **3**, 566 (1962).

[24] U. Khanal, Phys. Rev. D **28**, 1291 (1983).

[25] G. F. Torres del Castillo and G. Silva-Ortigoza, Phys. Rev. D **42**, 4082 (1990).

[26] W. H. Press and S. A. Teukolsky, Astrophys. J. **185**, 649 (1973).

[27] E. T. Newman and R. Penrose, J. Math. Phys. (N. Y.) **7**, 863 (1966).

[28] J. N. Goldberg, A. J. Macfarlane, E. T. Newman, F. Rohrlich and E. C. G. Sudarshan, J. Math. Phys. (N. Y.) **8**, 2155 (1967).

[29] V. Ferrari and B. Mashhoon, Phys. Rev. Lett. **52**, 1361 (1984).

[30] V. Ferrari and B. Mashhoon, Phys. Rev. D **30**, 295 (1984).

[31] S. Chandrasekhar, *The Mathematical Theory of Black Holes*, Oxford University Press, 1983.

[32] H. T. Cho, Phys. Rev. D **68**, 024003 (2003).